SUPPLEMENTAL MATERIAL

Hogstad et al., https://doi.org/10.1084/jem.20161881

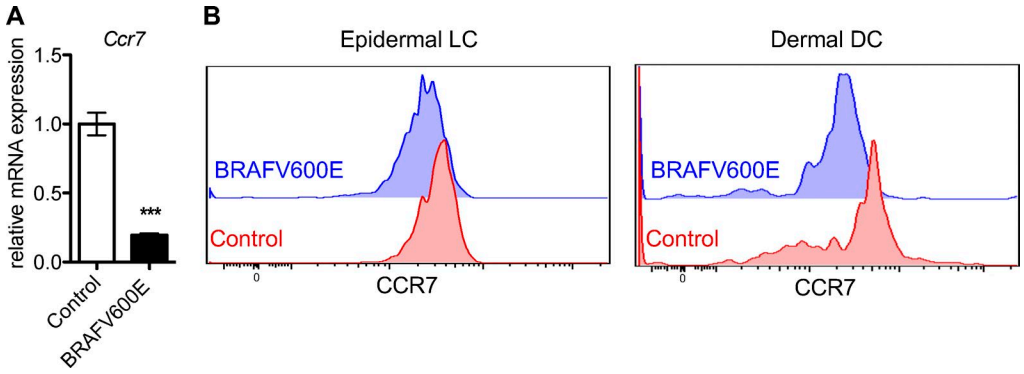

Figure S1. **Reduced CCR7 in *BRAF*V600E^{CD11c} spleen DCs and FITC-painted skin DCs. (A)** qPCR analysis of *Ccr7* mRNA levels in splenic CD11c^{+} DCs isolated by MACS CD11c-positive selection from control and *BRAF*V600E^{CD11c} mice (***, $P < 0.001$; unpaired *t* test). Results show the mean ± SEM from $n = 6$ mice. **(B)** *BRAF*V600E^{CD11c} or control mice were sensitized with FITC in the ears as described in the Materials and methods, and induction of CCR7 expression was measured in epidermal LC and dermal DC 16 h later. Histograms show CCR7 expression in epidermal Langerhans cells and dermal DCs ($n = 3–4$ mice per group).

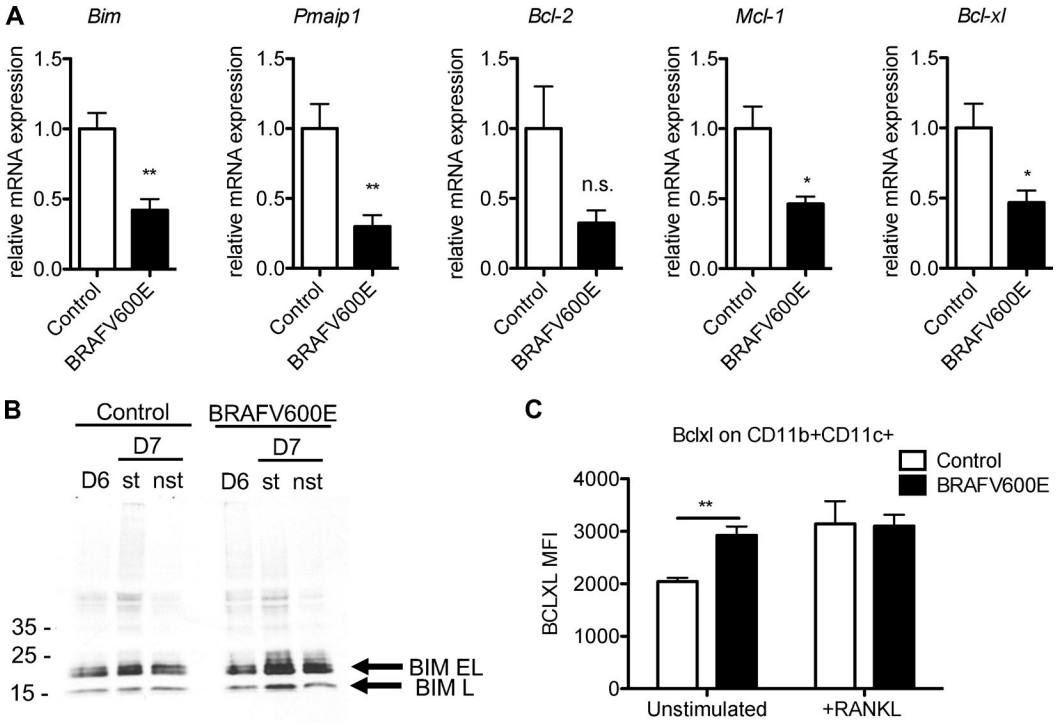

Figure S2. **Expression of pro- and antiapoptotic proteins in control and *BRAF*V600E DCs. (A)** CD11c^{+} splenocytes were isolated from *BRAF*V600E^{CD11c} or control mice and cultured for 6 h in standard medium then harvested for RNA extraction. mRNA levels for each listed pro or antiapoptotic molecule were measured by qPCR analysis and normalized to GAPDH (n = 6 mice in triplicate per group). **(B)** BIM (isoform BIM-EL and BIM-L) expression was measured by Western blots in *BRAF*V600E BMDCs starved (st) or not starved (nst) of GM-CSF growth factor in overnight culture. Representative data of two independent experiments are shown. Molecular mass is indicated in kilodaltons. **(C)** Control and *BRAF*V600E BMDCs were stimulated with RANKL overnight, stained for intracellular BCL-XL protein levels, then analyzed by flow cytometry. Results shown are representative of at least two independent experiments. Error bars indicate SEM (*, $P < 0.05$; **, $P < 0.01$; unpaired t test).

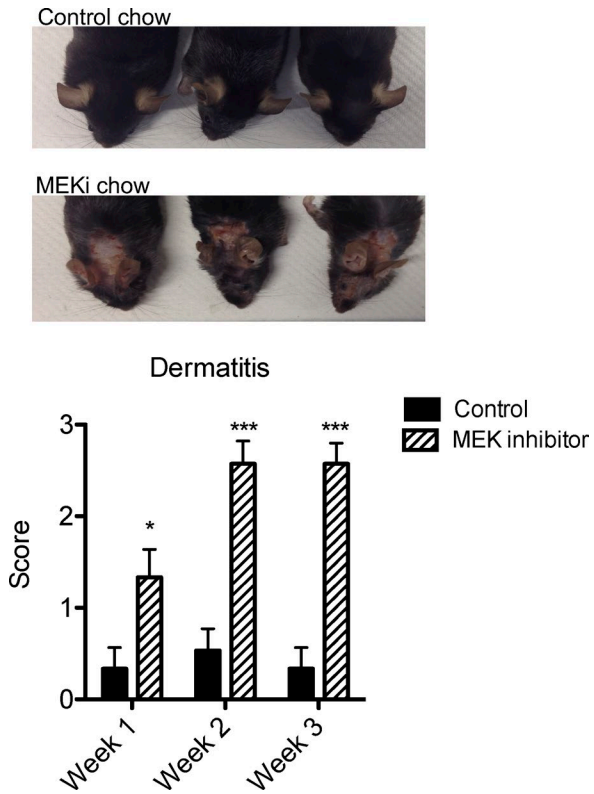

Figure S3. **Skin ulcerative lesions in mice treated with MEKi.** Dermatitis scores of *BRAF*V600E^{CD11c} chimeric mice after 1–3 wk of treatment with PD0325901 MEKi chow. Scale is 0–3 (0 is normal, 1 is visible punctate crusts, 2 is hair loss with merging crusts skin, 3 is ulcerated with hair loss). Data representative of at least two experiments with eight to nine mice per group are shown. Error bars indicate SEM (*, $P < 0.05$; ***, $P < 0.001$; unpaired *t* test).

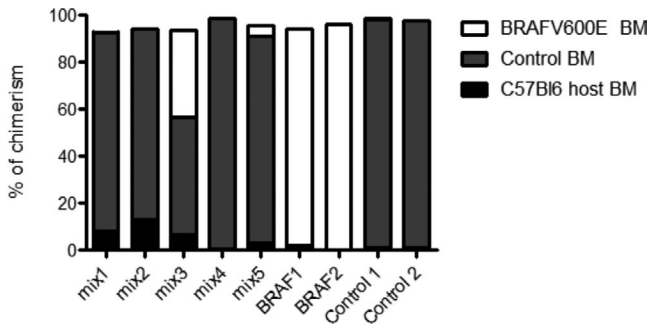

Figure S4. **Blood myeloid cell chimerism 4 wk after lethal irradiation and reconstitution by BM progenitors derived from *BRAF*V600E^{CD11c} mice and littermate controls reveals a competitive engraftment disadvantage of *BRAF*V600E^{CD11c} mice derived progenitors as compared with control BM progenitors.** Lethal irradiation of CD45.2 positive C57BL6/J mice with 2 × 600 rad followed by transplantation of 2×10^6 BM cells derived from CD45.1/2 double-positive *BRAF*V600E^{CD11c} mice (BRAF), CD45.1 control mice (Control) or both in a 1:1 ratio (mix). Bar plots show donor or host origin of CD11b$^+$ myeloid cells in the peripheral blood drawn 4 wk after transplantation as assessed by expression of CD45.1 and/or CD45.2 using multicolor flow cytometry analysis. Each column represents one mouse, representative of three independent experiments. Although we observed a satisfying reconstitution with a donor chimerism of >92% in mice reconstituted with BM from either *BRAF*V600E^{CD11c} mice or control mice, three mice of five reconstituted with mixed BM of both backgrounds displayed only donor cells derived from the control BM. In one mouse, only 4.7% of CD11b$^+$ myeloid cells in the blood stained positive for the congenic marker of *BRAF*V600E^{CD11c} mice, and in only one mouse, donor chimerism of 37.1% from *BRAF*V600E^{CD11c} mice could be established.

Table S1. **Tissue slide details for LCH samples from Fig. 1 F**

Diagnosis	Mutation	Tissue	Gender	Risk	Single/multiple lesions	Single system versus multisystem	CNS risk	Diabetes insipidus	Recurrent
LCH	V600E	LN	Female	HR	Multiple	Multisystem	Yes	No	Yes
LCH	V600E	LN	Female	HR	Multiple	Multisystem	Yes	No	Yes
LCH	V600E	Soft tissue left orbit	Male	LR	Single	Single	Yes	No	No

CNS, central nervous system; HR, high risk; LR, low risk.

Table S2. **LCH lesion details for specimens used in Figs. 2 and 3**

Patient ID	Age	Gender	Disease	Sites of LCH Lesions
	yr			
BRAF V600E	17.26	Male	LCH	Frontal bone (single lesion)
BRAF V600E	2.2	Male	LCH	Temporal bone, frontal bone ×2, mastoid, cerebellar T2 hyperintensity
BRAF V600E	0.61	Female	LCH	Multifocal bone (temporal bone, mastoid), skin, ears
BRAF V600E	1.11	Female	LCH	Skin, multifocal bone (mandible, parietal skull, left ilium, T1, T4,9,12; L1,3,4, pelvis, bilateral humeri and femori, spleen, liver, skin, LNs, lung, ears)
WT BRAF	16.37	Male	LCH	Lungs, skin, pituitary
WT BRAF	5.66	Male	LCH	Occipital bone (single lesion), possible skin
WT BRAF	4.46	Female	LCH	Ischium (single lesion)
MAP2K1 (302-303)	2.87	Female	LCH	Multifocal bone: orbit, parietal bone, femurs (bilateral), spine (C1, T10)